CrossMark

Low molecular weight fucoidan ameliorates the inflammation and glomerular filtration function of diabetic nephropathy

Yingjie Xu [1,2,3] · Quanbin Zhang [1,4,5] · Dali Luo [6] · Jing Wang [1,4] · Delin Duan [1,4,5]

Abstract Diabetic nephropathy (DN) is a type of serious microangiopathy that is caused by diabetes mellitus (DM). It is the most common cause of chronic renal failure and end-stage renal disease, and it severely affects patients' quality of life. This work aims to study the effect and mechanism of low molecular weight fucoidan (LMWF) on streptozotocin (STZ)-induced DN. The experimental results showed that LMWF prevented weight loss in DN rats, significantly reduced the levels of biochemical indexes in blood and urine samples, and also lowered hyaluronic acid (HA) levels and advanced glycosylation end product-specific receptor (AGER) levels in DN rats. LMWF maintained the structural integrity of glomerular basement membrane (GBM) and glomerulus, improved the glomerular filtration function, protected glycosaminoglycan from abnormal degrading, prevented advanced glycosylation end product (AGE) from being generated and accumulating, and also alleviated inflammatory response in DN rats. LMWF could obviously ameliorate and slow the development and progression of DN in rats.

✉ Quanbin Zhang
qbzhang@qdio.ac.cn

✉ Delin Duan
dlduan@qdio.ac.cn

1   Key Lab of Experimental Marine Biology, Institute of Oceanology, Chinese Academy of Sciences, Qingdao 266071, China

2   Institute of Cerebrovascular Diseases, Affiliated Hospital of Qingdao University, Qingdao 266003, China

3   University of the Chinese Academy of Sciences, Beijing 100049, China

4   Lab for Marine Biology and Biotechnology, Qingdao National Lab for Marine Sci. & Tech, Qingdao 266071, China

5   State Key Lab of Seaweed Bioactive Substances, Qingdao, China

6   Department of Pharmacology, School of Chemical Biology & Pharmaceutical Sciences, Capital Medical University, Beijing 100069, China

Introduction

Diabetes mellitus (DM) is a set of multifactorial metabolic disorders that is characterized by hyperglycemia (Naylor et al. 2011). The incidence of DM has increased rapidly and become a major health problem worldwide (Group IDFDA 2015). According to International Diabetes Federation, the number of diabetic patients is expected to rise to 592 million by 2035 (Nyla Nazir et al. 2014). DM is the leading cause of a number of vascular complications, including renal, cardiovascular, and retinal and many other comorbidities (Vlassara and Striker 2011). Diabetic nephropathy (DN) is a type of serious microangiopathy caused by DM. According to World Health Organization, 25–40 % of type 1 or type 2 diabetic patients will develop DN within the course of diabetes over 20–25 years (Remuzzi et al. 2002; Yamagishi and Matsui 2010). Currently, DN is the major cause of chronic renal failure and end-stage renal disease (Terami et al. 2014); it severely affects patients' quality of life. Long-term hyperglycemia leads to the formation of advanced glycation end products (AGE) (Singh et al. 2014), resulting in the thickening of the glomerular basement membranes (GBM), glomerular hardening and fibering, mesentery expanding, as well as other features (Li et al. 2010). Many cytokines are related to the onset and progression of DN. And some inflammatory cytokines, such as vascular endothelial growth factor (VEGF), connective tissue growth factor (CTGF), interleukin-6 (IL-6), as well as numerous other

factors, can mediate inflammation in DN (Kanwar et al. 2011; Matsushita et al. 2011; Lim and Tesch 2012; Kanasaki et al. 2013; Sawa et al. 2014).

Fucoidan is a family of sulfated polysaccharides composed of an α-L-fucose-enriched backbone and exists extensively in brown algae and a few marine invertebrates (Jiao et al. 2011; Cui et al. 2014). Fucoidans isolated from brown algae have very complicated and heterogeneous structures, while fucoidans often have a simple repeat unit structure in marine invertebrates (Wang et al. 2010b). Fucoidans have a wide range of biological activities, and because of their complex heteropolysaccharide structure, the activity of fucoidans may vary in different species and orders of algae (Costa et al. 2010; Wang et al. 2010b; Wijesekara et al. 2011). Saccharina japonica is a prevalent seafood and traditional Chinese medicine that has been used in Asia for several centuries (Wang et al. 2012). Fucoidan obtained from S. japonica is a heteropolysaccharide composed of fucose, galactose, and sulfate, with a small number of mannose, glucuronic acid, glucose, rhamnose, arabinose, and xylose units (Wang et al. 2008). Low molecular weight fucoidan (LMWF) is a highly sulfated fraction that is degraded from fucoidan from S. japonica (Wang et al. 2008; Jin et al. 2013). Studies have demonstrated that the biological activities of polysaccharides are relative to the degree of sulfation, molecular weight, sulfation pattern, and glycosidic branches (Wang et al. 2010a). As a result of these characteristics, LMWF has strong anticoagulant (Nardella et al. 1996; Durig et al. 1997), anti-inflammatory (Bachelet et al. 2009), antiangiogenic (Deux et al. 2002; Hlawaty et al. 2011), antiviral (Hemmingson et al. 2006), antithrombus (Durand et al. 2008; Zhu et al. 2010), antioxidant (Wang et al. 2011b; Yu et al. 2014), and antitumor (Anastyuk et al. 2012; Zhang et al. 2013) activities and modulates cell adhesion (Bachelet et al. 2009) and growth factor release (Chen et al. 2013).

The glomerular barrier is one of the most complex and unique biological membranes and serves as the key component in the filtration of water and restricts the passage of large molecule proteins (Haraldsson et al. 2008). The GBM plays a central role in the glomerular filtration barrier (Singh et al. 2007; Satchell and Braet 2009), heparan sulfate proteoglycans (HSPGs) are essential proteoglycans located in the GBM and other membranes, and they are composed of a core protein and several heparan sulfate glycosaminoglycan chains (HS-GAGs) (Bishop et al. 2007). It is generally believed that HS-GAGs are important for the charge selectivity function of the barrier because of the anionic charge of heparan sulfate (HS). HSPGs establish the charge barrier on the GBM to regulate solutes (McCarthy and Wassenhove-McCarthy 2012).

Therefore, losing of GBM anionic charge contributed by HS-GAGs will produce proteinuria, which is an important clinical feature of DN, followed by further effects of DN (Sakagami et al. 2004; Takahashi et al. 2006).

Because of the composition of LMWF is similar to HS-GAGs, both LMWF and HS-GAGs have sulfation pattern and glycosidic branches; LMWF may be contribute to the restoration of GBM. Moreover, the progression of DN is related to inflammatory cytokines, and LMWF has strong and efficacious anti-inflammatory activities. And our previous study demonstrated that fucoidan (87,000 Da) showed protective properties to the kidney of DN rats (Wang et al. 2014).

Various factors contribute to DN, such as renal fibrosis and inflammation. Inhibition of diabetic renal fibrosis supports a beneficial effect to DN (Tomita et al. 2012; Kanasaki et al. 2013). Sulodexide and low molecular weight heparin which have anticoagulant and antithrombotic activities are effective in reducing the early chronic kidney disease (Rossini et al. 2010; Fan et al. 2012). AGEs participate in the generation of reactive oxygen species. And oxidative stress can activate many signal pathways, such as MAPK pathway; it can injure the renal tissue seriously (Pal et al. 2014). Therefore, interruption and inhibition of the signaling pathway leading to the production of reactive oxygen can ameliorate DN (Kashihara et al. 2010). Furthermore, LMWF has strong activities of anticoagulant, antifibrotic, and antioxidant and so on. As a consequence, it was suggested that LMWF could be considered a potential anti-diabetic nephropathy candidate.

In this study, we focus on the anti-inflammatory of LMWF. Because of these properties, we hypothesize that LMWF can protect the glomerular filtration function and modulate the release of inflammatory factors in DN. This work aims to study the effect and mechanism of LMWF on DN in vivo experimental models.

Materials and methods

Saccharina japonica were cultured by one of the authors (D.D.) in Rongcheng, China. Specimens of S. japonica were collected and identified by one of the authors (D.D.). LMWFs (molecular weight = 8177 Da) were isolated from S. japonica. The analysis was as follows: fucose content 35.07 %, sulfate content 36.85 %, and uronic acid content 0.039 %. The polysaccharide was a single compound authenticated by high-performance liquid chromatography and capillary electrophoresis. The structure of LMWF was determined by monosaccharide composition analysis, methylation analysis, periodate oxidation, smith degradation, and many other tests (Wang et al. 2010b).

Table 1 Primary antibodies used for staining

Antibody	Source	Company	Dilution (IHC/WB)
CTGF	Rabbit	Proteintech	1:100/1:2000
VEGF	Rabbit	Proteintech	1:100/1:2000
AGER	Rabbit	Proteintech	1:100/1:2000
IL-6	Rabbit	Proteintech	1:100/1:2000
Icam-1	Rabbit	Proteintech	1:100/1:2000
TGF-β	Rabbit	ThermoFisher-Pierce	1:100/1:2000
TNF-α	Rabbit	ThermoFisher-Pierce	1:100/1:2000
PDGFRβ	Rabbit	ThermoFisher-Pierce	1:100/1:2000
JNK	Rabbit	Proteintech	1:100/1:2000
P-JNK	Rabbit	Proteintech	1:2000
PKCβ	Rabbit	Proteintech	1:100/1:2000

Captopril tablets were purchased from the Harbin Pharmaceutical Group. All primary antibodies are summarized in Table 1. The Polink-2 plus polymer horseradish peroxidase (HRP) detection system kit and DAB protein assay kit were from GBI, USA. The urinary albumin (uAlb) and urinary creatinine (uCr) enzyme-linked immuno sorbent assay (ELISA) kits were from Bo Maide Co., Ltd., Shanghai, China. Streptozotocin (STZ) was from Sigma-Aldrich, China. All drugs were dissolved in normal saline, unless otherwise noted.

Animals

Wistar male rats, weighting approximately 180–220 g, were from the Laboratory Animal Center, Shandong University, China, and reared in a standard conditions for experimental animals: room temperature = 22 ± 1 °C, humidity = 60 ± 5 % and a 12-h light/12-h dark cycle. The animals were fed with normal food and water ad libitum.

All of the rats were fed adaptively for 1 week, and then the DM model was induced by STZ (50 mg kg^{-1} day^{-1}) and administered by intraperitoneal injection. Forty-eight hours later, the blood glucose levels from the caudal vein were detected for 3 days. Rats with blood levels >16.7 mmol L^{-1} were considered as successful DM models. Model rats were randomly divided into five groups (18 rats per group): (1) the normal group (Wistar normal rats); (2) the LMWF (100 mg) group, rats were treated with LMWF 100 mg kg^{-1} day^{-1}; (3) the LMWF (200 mg) group, rats were treated with LMWF 200 mg kg^{-1} day^{-1}; (4) the captopril (10 mg) group, rats were treated with captopril 10 mg kg^{-1} day^{-1} (Yamagishi and Matsui 2010; Zhang et al. 2012; Pan et al. 2014); and (5) the model group (DM model rats). All of the groups were orally administered the drug between 08:00 and 10:00 h for 70 days. Meanwhile, the rats in the normal and model groups were treated with equal volumes of saline.

Body weights were measured approximately every 5 days, and 24-h urine samples of all rats were collected on the 35th day and 1 day before sacrifice by metabolism cages. The blood samples of all rats were drawn from orbit on 35th day and 1 day before sacrifice. All rats were sacrificed on the 70th day. The rats were anesthetized with 0.3 mL (100 g)$^{-1}$ 10 % chloral hydrate. Kidneys of all rats were removed and frozen by liquid nitrogen and fixed in 4 % paraformaldehyde respectively for the following tests.

The analysis of urinary M-TP

Twenty-four-hour urine samples of all groups were collected and centrifuged, and the supernatants were transferred to clear collection tubes. Then, the total volumes of the 24-h urine samples were measured and recorded. Afterwards, supernatants of 24-h urine sample were sent for detection. The micrototal protein (M-TP) was detected by an automatic biochemistry analyzer AU5800 (Beckman Coulter, USA).

UAlb and uCr levels assessed by ELISA

Twenty-four-hour urine samples from all groups were collected by sterile tubes. The specimens were centrifuged at 3000 rpm for 20 min at room temperature. The supernatants were removed into rat uAlb and uCr ELISA kit plates respectively in accordance with the manufacturers' protocols. The OD values of the uAlb and uCr levels from of all groups were determined at 450 nm by an automatic microplate reader (BioTek Instruments Inc., USA).

The analysis of the serum biochemical index

Blood samples were taken from the orbit and collected into different type of tubes to detect blood biochemical indices, including blood glucose (GLU), urea nitrogen (UREA), serum creatinine (CREA), total cholesterol (CHOL), triglyceride (TRIG), high-density lipoprotein cholesterol (HDL-C), low-density lipoprotein cholesterol (LDL-C), and glycated serum protein (FRUC). All blood samples were assessed with an automatic biochemistry analyzer AU5800 (Beckman Coulter, USA).

Glycosaminoglycan measurements using the 1, 9-dimethyl methylene blue assay

The glycosaminoglycan levels of the urine samples were measured by ELISA assay. One hundred-microliter samples were added to 96-well plates; 200 μL 1, 9-dimethyl

methylene blue (DMMB) solution (Sigma-Aldrich) was also added into the wells to bind to the sulfated glycosaminoglycan in the samples. The hyaluronic acid (HA) and chondroitin sulfate (CHS) levels were determined using the DMMB dye method (Wang et al. 2011a). CHS from shark cartilage and HA from *Streptococcus equi* (Sigma-Aldrich) were used as the standard. The OD values of the CHS and HA from all groups were detected at 520 nm using an automatic microplate reader.

The histological analysis of sections of renal pathological changes

Kidneys from all groups were removed and fixed in 4 % para-formaldehyde. The fixed kidneys were dehydrated using graded saccharose at 4 °C. After complete dehydration, all kidneys were frozen in liquid nitrogen and embedded with OCT compound (Sakura, USA). The embedded tissues were formed into 10 μm thick frozen sections for the following tests.

Histological evaluations were performed with hematoxylin and eosin (HE) staining. Frozen sections from all groups were stained using HE methods, with hematoxylin for 5 min and eosin for 1 min. The histological analysis and the areas of inflammatory infiltration of the kidneys were assessed with an optical microscope.

The sub-microstructure analysis of the GBM

Parts of the renal cortices were trimmed into 1 mm^3 bars and fixed in 2.5 % glutaraldehyde at 4 °C. Ultrathin sections of the renal cortex were made and double stained with uranyl acetate and sodium citrate at the Medical College of Qingdao University. Glomerulus-centered sub-microstructure was observed by transmission electron microscope (TEM). GBM thickness of the different groups was measured.

Immunohistochemistry examination

Frozen sections were washed for 5 min with Tris-HCl buffer solution (TBS), and preprocessed for 10 min with a 3 % hydrogen peroxide solution to inactivate endogenous peroxidase. The primary antibodies (CTGF, VEGF, advanced glycosylation end product-specific receptor (AGER), IL-6, intercellular adhesion molecule-1 (Icam-1), transforming growth factor-β (TGF-β), tumor necrosis factor-α (TNF-α), platelet-derived growth factor β (PDGFRβ), c-Jun amino terminal kinase (JNK), and protein kinase Cβ (PKCβ)) are described in Table 1) were added onto sections respectively for 12 h at 4 °C and then washed twice for 5 min with TBS. A HRP-labeled secondary antibody polymer was attached onto sections in accordance with the kit's protocol. The stained sections were dehydrated in a series of decreasing concentrations of ethanol solutions and were mounted with neutral balsam. The immunoreactivity of all antibodies and the numbers of positive cells in all groups were measured by Image-Pro Plus 6.0 software.

Western blotting

Kidney tissue was lysed on ice in RIPA buffer contain phenylmethanesulfonyl fluoride for 20 min and total protein content was quantified using a BCA assay kit. Lysates were separated by 12 % sodium dodecyl sulfate-polyacrylamide gel electrophoresis and carried out in triplicate. Proteins on the gel were blotted to polyvinylidene difluoride membranes (Solarbio Science & Technology Co., Ltd., China). Blotted membranes were incubated overnight with primary antibody at 4 °C (see CTGF, VEGF, JNK, and P-JNK in Table 1). Then, peroxidase-conjugated goat anti-rabbit secondary antibody (Proteintech Group Inc., China) was added to the immunoblotted membranes for 2 h. Blotted bands were revealed using an ECL kit and the bands was analyzed.

Data analysis and statistics

All data are expressed as the means ± S.D. The images were processed by Image-Pro Plus 6.0 software. Multiple comparisons between treatment groups and the statistical significance of the differences were estimated with ANOVA method using SPSS 13.0 software, and values of $P < 0.05$ were considered to be statistically significant.

Results

Evaluation of rats weight alteration in two terms

Body weight changes of all rats were examined in both stages (Fig. 1). Significant changes in body weight were observed between the normal and other groups during the treatment period. The body weight of the normal group was significantly higher ($P < 0.01$), while the body weight of the model group was significantly lower compared to other treatment groups. In addition, the body weight of the LMWF (200 mg) group was higher than the that of captopril (10 mg) and LMWF (100 mg) groups. Compared to the model group, the body weight of LMWF (200 mg) group showed a noticeable rise. The result indicates that LMWF may maintain body weight more stable during the onset of DN in rats.

Effects of LMWF on M-TP, uAlb, and uCr in DN rats

Proteinuria is the most outstanding feature of DN. We detected the M-TP, uAlb, and uCr levels of all groups. The urinary M-TP content was significantly lower ($P < 0.01$) in the normal group and was higher ($P < 0.01$) in the model group in both
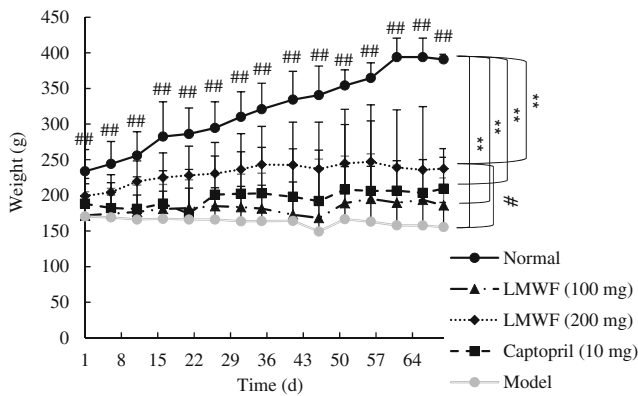
Fig. 1 Body weight of different treated groups after 70 days. Data are expressed as means ± S.D. *Double asterisk* $P < 0.01$ (vs normal group); *hash* $P < 0.05$, *double hash* $P < 0.01$ (vs model group)

stages (Fig. 2a). The M-TP content of the LMWF (100 mg) and LMWF (200 mg) groups was reduced compared to the model group at 35 days, and the M-TP content of the LMWF and captopril (10 mg) treatment groups were nearly the same and ameliorated compared to that of the model group at 69 days. The 24-h urine volumes of LMWF (100 mg), LMWF (200 mg), captopril (10 mg), and model groups were significantly increased compared to those of the normal group (Fig. 2b), and the 24-h urine volume of LMWF (200 mg) group was obviously reduced compared to the model group at 35 days. LMWF, especially for the LMWF (200 mg) group, can reduce urine volume at the onset of DM in rats compared to the model group.

Next, we determined the uAlb and uCr levels to further verify the effect of LMWF on the glomerular filtration function (Fig. 3) at two stages. The uAlb level was significantly lower ($P < 0.01$) in the normal group and higher ($P < 0.01$) in the model group. LMWF obviously reduced the uAlb levels compared to those of the model group at 35 days, but there were no statistical differences among groups at 69 days. And LMWF had no evident influence on the uCr levels. The results demonstrated that LMWF can alleviate the M-TP content and uAlb levels in DN rats, especially in early stage of DN.
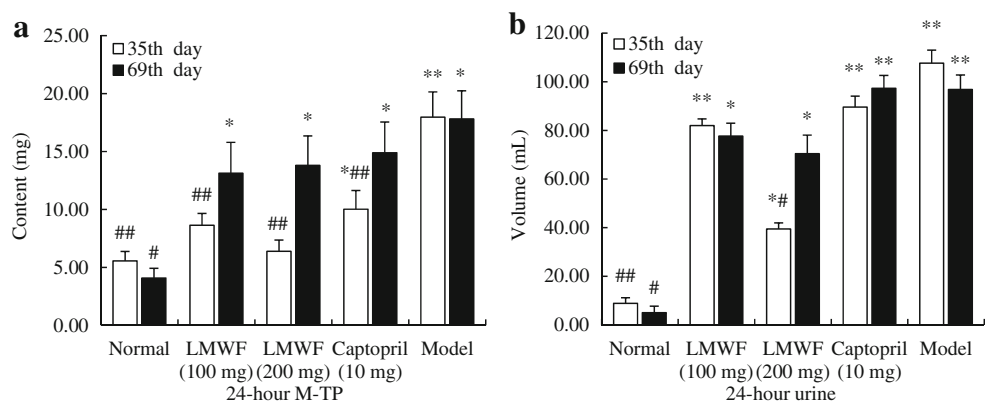
Effects of LMWF on the serum biochemical indexes in diabetic rats

The serum biochemical analysis showed that LMWF did not affect most indices, such as CHOL, TRIG, CREA, HDL-C, and LDL-C. There were no significantly differences in these indices compared to the normal groups. However, GLU, UREA, and FRUC, the main signs of DN, obvious intergroup differences were observed, regardless of the comparison with the normal or model group.

The GLU level was significantly lower ($P < 0.01$) in the normal group and higher ($P < 0.01$) in other groups (Fig. 4a). The GLU levels of the LMWF (200 mg) and captopril (10 mg) group were basically the same, lower than that of the model group.

The UREA level was significantly lower ($P < 0.01$) in the normal group and was higher ($P < 0.01$) in the model group (Fig. 4b). The UREA level of the LMWF (200 mg) group was more ameliorated ($P < 0.05$) than that of the captopril (10 mg) and model groups. The effect of LMWF at 35 days was more remarkable than that at 69 days.

The FRUC level was also significantly lower ($P < 0.01$) in the normal group compared to that of the other groups (Fig. 4c). At 35 days, the FRUC level of the LMWF (200 mg) group was ameliorated ($P < 0.01$) obviously compared to that of the model group. However, at 69 days, the UREA levels were ameliorated in the LMWF (200 mg) and captopril (10 mg) groups. Moreover, the effect of LMWF (100 mg) on the GLU, UREA, and FRUC levels were not significant compared to the model group. The results indicated that LMWF (200 mg) could effectively reduce the UREA and FRUC levels in DN rats. And those significant differences between the normal and model group meant the DM models were established successfully.

Effects of LMWF on glycosaminoglycan levels in DN rats

To confirm the protective effects of LMWF on rat kidneys, the HA and CHS levels, which are two typical glycosaminoglycans

Fig. 2 LMWF reduced urinary M-TP level in 70 days. **a** The content of 24-h M-TP in all groups. **b** The volume of 24-h urine in all groups. Data are expressed as means ± S.D. *Asterisk* $P < 0.05$, *double asterisk* $P < 0.01$ vs (normal group); *hash* $P < 0.05$, *double hash* $P < 0.01$ (vs model group)
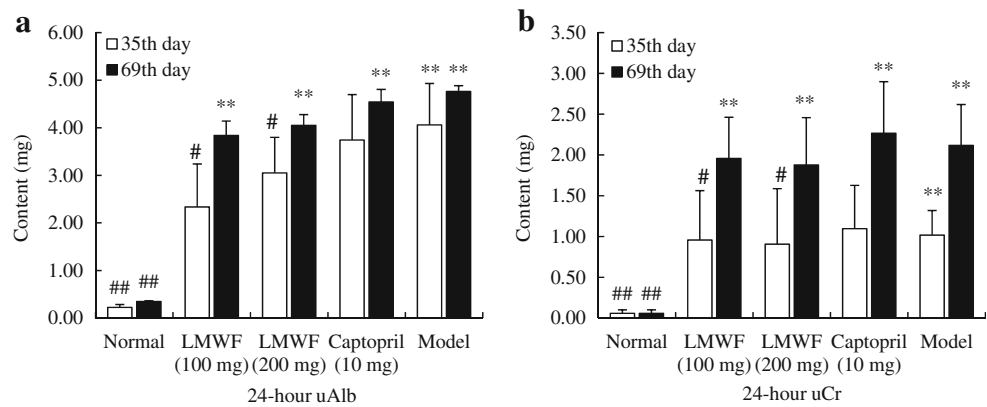
in the urine were inspected (Fig. 5). The HA at two stages remained statistically lower in the normal group ($P < 0.01$) compared to the other groups, while the level in the model group remained higher ($P < 0.01$). And the LMWF-treated groups reduced the HA levels compared to the model group ($P < 0.05$). However, for CHS, no significant regularity was found between the different groups. These results illustrated that LMWF could lower HA levels in DN rats.

Renal function and the histopathological analysis

Representative histopathological sections of all groups are presented in Fig. 6. Normal and compact structured glomerulus and tubules were observed in rats in the normal group.

Both the glomerulus and tubules exhibited severe structural damage in the model groups; rats in the LMWF (200 mg) group had relatively normal and complete glomerulus and tubules structure; and partially dilated glomerulus were found in the captopril (10 mg) group accompanied by mild kidney damage ($P < 0.01$); however, almost all of the glomerulus were dilated and the epithelial cells were denuded in the LMWF (100 mg) group. Compared to the model group, the area of the inflammatory infiltration of LMWF-treated groups was much less and showed a return to basal level. These results revealed that LMWF could inhibit and improve pathological changes in the kidneys of DN rats.

To further clarify the effect of LMWF on glomerulus, we measured GBM thickness by transmission electron microscope
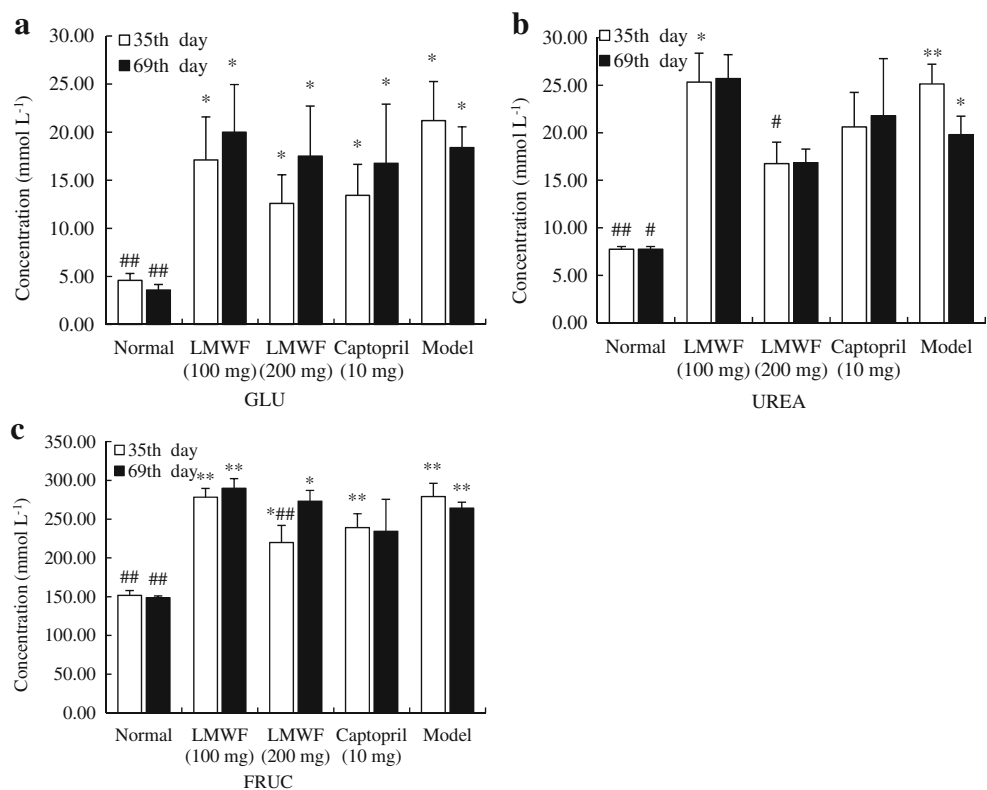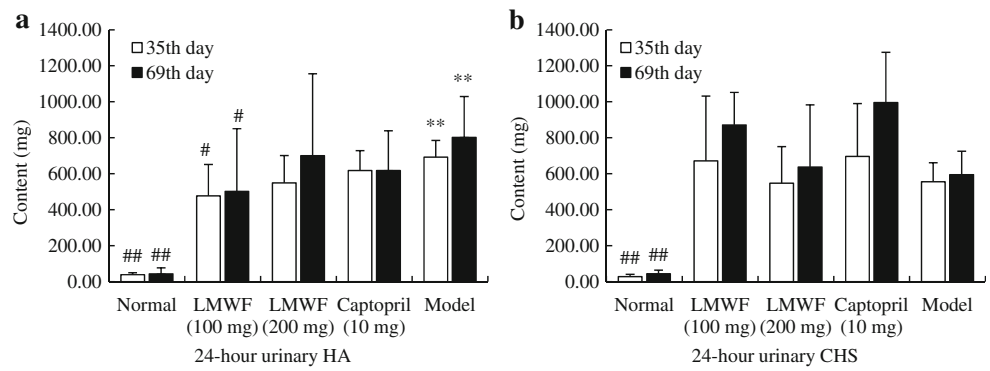
Fig. 5 Effect of LMWF on urinary glycosaminoglycan levels by DMMB assay in DN rats in 70 days. **a** The 24-h urinary HA levels and **b** the 24-h urinary CHS levels were measured respectively. Data are expressed as means ± S.D. *Double asterisk P* < 0.01 (vs normal group); *hash P* < 0.05, *double hash P* < 0.01 (vs model group)

(Fig. 7). The GBM was significantly thinner ($P < 0.01$) in the normal group and thicker ($P < 0.01$) in the model group. The LMWF (200 mg) ($P < 0.05$) groups had notably inhibited GBM widening and restrained mesentery proliferating, compared to the model group. Additionally, the GBM in the LMWF (100 mg) and captopril (10 mg) groups were modified, compared to the model group. These results suggested that LMWF could inhibit GBM thickening and relieve pathological changes in the kidneys of DN rats to improve the glomerular filtration function.

### Effects of LMWF on AGER in DN rats

AGER, a multiligand receptor of AGE, is an important factor in DN. Our results showed that LMWF could effectively reduce the AGER levels in the kidneys of DN rats (Fig. 8). The AGER level of the normal group remained significantly lower ($P < 0.01$), and the level were higher ($P < 0.01$) in the model

group, while LMWF treatment suppressed the elevated AGER expression in DN rats compared to the model group ($P < 0.01$). These results indicated that LMWF could suppress the generation and depositing of AGER in the kidneys of DN rats.

Effects of LMWF on inflammatory cytokines in DN rats

Several cytokines were examined by immunohistochemistry to investigate the effects of LMWF on inflammatory cytokines (Fig. 9). No statistical alterations were observed in the Icam-1, TNF-α, PDGFRβ, TGF-β, and PKCβ expression. However, compared to the model group, LMWF significantly alleviated the positive expression of JNK, IL-6 and VEGF in the kidneys of DN rats. LMWF (100 mg) reduced the positive expression of JNK and IL-6 ($P < 0.01$) lower than LMWF (200 mg); both LMWF (100 mg) and LMWF (200 mg) suppressed the
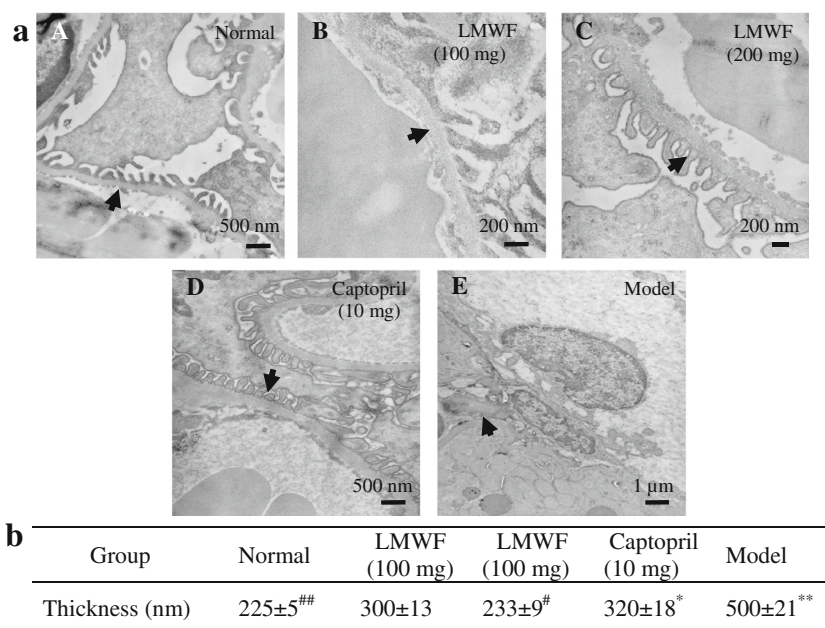
Fig. 6 LMWF improves glomerulus pathological change of DN rat kidneys. **a** (*A*) Representative images of the normal group by H&E staining, (*B*, *C*) groups administered with LMWF at doses of 100 and 200 mg kg^{-1} day^{-1} respectively, (*D*) captopril (10 mg) group, and (*E*) model group. *Black arrows* indicate glomerulus has clearly morphological characteristics (original magnification ×800). *Scale bar* = 25 μm in each panel. **b** Areas of inflammatory infiltration were estimated in five visual fields in one section. Data are expressed as means ± S.D. *Asterisk P* < 0.05, *double asterisk P* < 0.01 (vs normal group); *hash P* < 0.05, *double hash P* < 0.01 (vs model group)
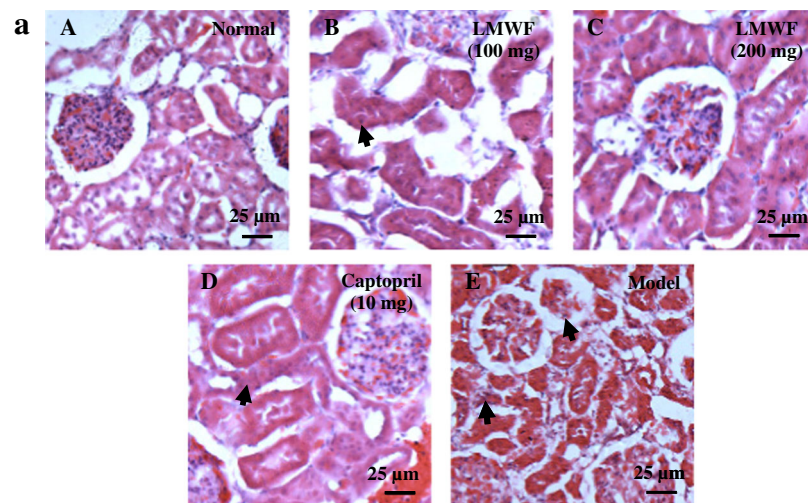
Areas of inflammatory infiltration (μm^2)	Normal	LMWF (100 mg)	LMWF (200 mg)	Captopril (10 mg)	Model
35th day	25.25±10.00##	800.15±53.75*#	575.15±75.25#	700.65±175.55*#	1575.95±175.70**
69th day	158.50±25.00##	1125.05±105.25*#	850.35±127.75#	1025.55±125.55*#	2325.15±225.75**

Fig. 7 LMWF inhibits GBM thickening in DN rat kidneys. **a** Representative images of all groups by TEM. (*A*) Normal group, (*B*, *C*) groups administered with LMWF at doses of 100 and 200 mg kg^{-1} day^{-1}, (*D*) captopril (10 mg) group, and (*E*) model group. *Black arrows* indicate GBM has clearly morphological characteristics. *Scale bar* = 500 nm in *panels A* and *D*. *Scale bar* = 200 nm in *panels B* and *C*. *Scale bar* = 1 μm in *panel E*. **b** GBM thickness of different groups. Data are expressed as means ± S.D. *Asterisk P* < 0.05, *double asterisk P* < 0.01 (vs normal group); *hash P* < 0.05, *double hash P* < 0.01 (vs model group)

Group	Normal	LMWF (100 mg)	LMWF (100 mg)	Captopril (10 mg)	Model
Thickness (nm)	225±5##	300±13	233±9#	320±18*	500±21**

positive expression of VEGF ($P < 0.01$). These results demonstrated that LMWF could ameliorate cytokine expression.

To further confirm the effect of LMWF on the key molecules, we detected the protein expression levels of CTGF, VEGF, JNK, and P-JNK by western blot (Fig. 10). Results showed the expressions of CTGF, VEGF, JNK, and P-JNK in model group were much higher than that of normal group. LMWF obviously reduced the expression of those key factors compared to model group.

CTGF was restained with hematoxylin after immunohistochemistry, and positive cells were counted to determine the CTGF expression level (Fig. 11). Compared to the other groups, the number of positive cells was much lower in the normal group and was much higher in the model group. The number of positive cells in the LMWF (200 mg) groups was significantly lower, and in LMWF (100 mg) group, the number was also statistical lower compared to the model group.
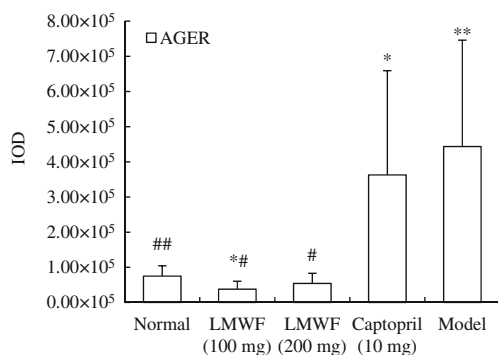

Fig. 8 LMWF reduced AGER level on kidney of DN rats. Data are expressed as means ± S.D. *Asterisk P* < 0.05, *double asterisk P* < 0.01 (vs normal group); *hash P* < 0.05, *double hash P* < 0.01 (vs model group)

These results showed that LMWF could ameliorate the CTGF level in the kidneys of DN rats.

Discussion

The results reported in the present work demonstrated the influence of LMWF in DN rats induced by STZ, and proposed a possible method to illustrate the mechanism of the effect of LMWF on DN; it may be a potential therapy in the future.

Currently, M-TP and uAlb are the only noninvasive hallmarks of early diabetic nephropathy; uCr is a marker of mid-to-late disease (Papale et al. 2010). These markers reflect the progression of DN. Clinically, uAlb reflects the loss of the glomerular filtration function and podocyte injury (Ma et al. 2014) and shows a set of changes, such as basement membrane thickening, loss of endothelial cell fenestration and mesangial cell hypertrophy, coupled with tubulointerstitial changes, such as myofibroblast accumulation and fibrosis (Weil et al. 2012). In our study, we detected the levels of all three indices in both blood and urine samples of all rats. Compared to normal group, there were significant changes in model group; it means the DM model were established successfully. LMWF could decrease the content of M-TP and uAlb in the urine (Figs. 2, 3, and 4). Additionally, LMWF, especially LMWF (200 mg kg^{-1}), may prevent abnormal weight loss and decrease urine volume (Figs. 1 and 2a). Captopril (10 mg kg^{-1}) is the preferred drug to reduce the urine protein and slow the decline rate of renal function without influence blood sugar level, so we used the captopril as the positive contrast drug. The GLU levels of the LMWF (200 mg) group and captopril (10 mg) group were basically the same. Previous study has demonstrated that LMWF
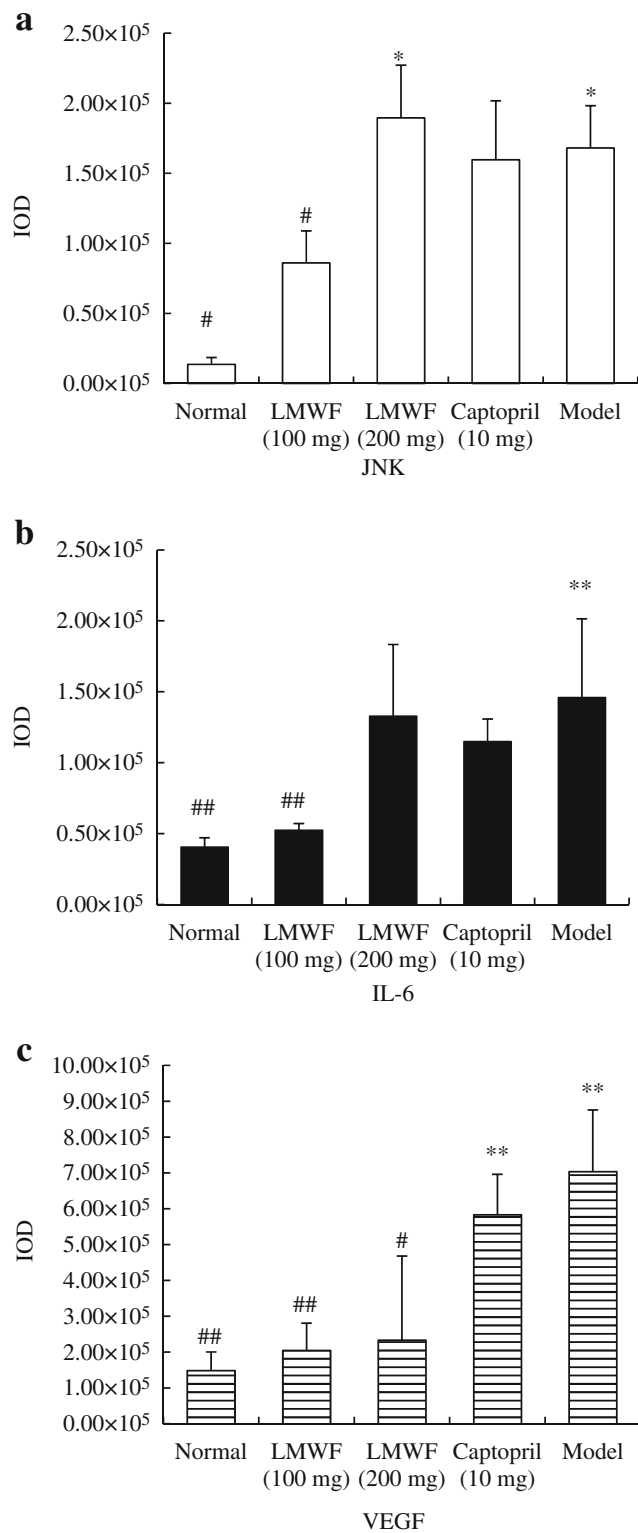
a

b

c

Fig. 9 LMWF decreased inflammatory cytokines expression by immunohistochemistry. Positive expression was detected by IPP 6.0. **a** JNK level of all groups. **b** IL-6 level. **c** VEGF level. Data are expressed as means ± S.D. *Double asterisk P < 0.01* (vs normal group); *hash P < 0.05, double hash P < 0.01* (vs model group)
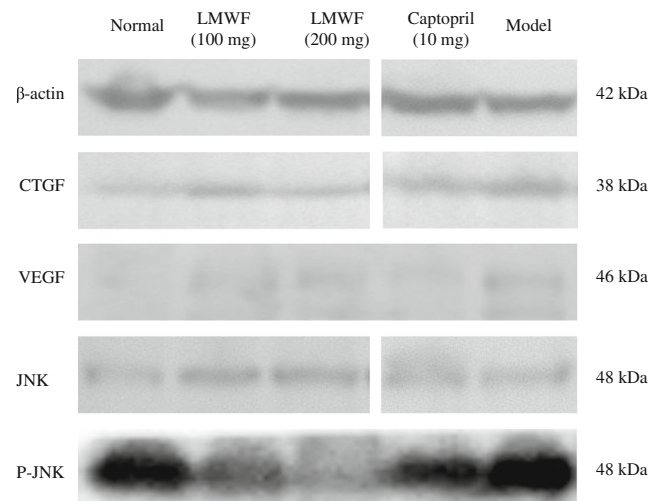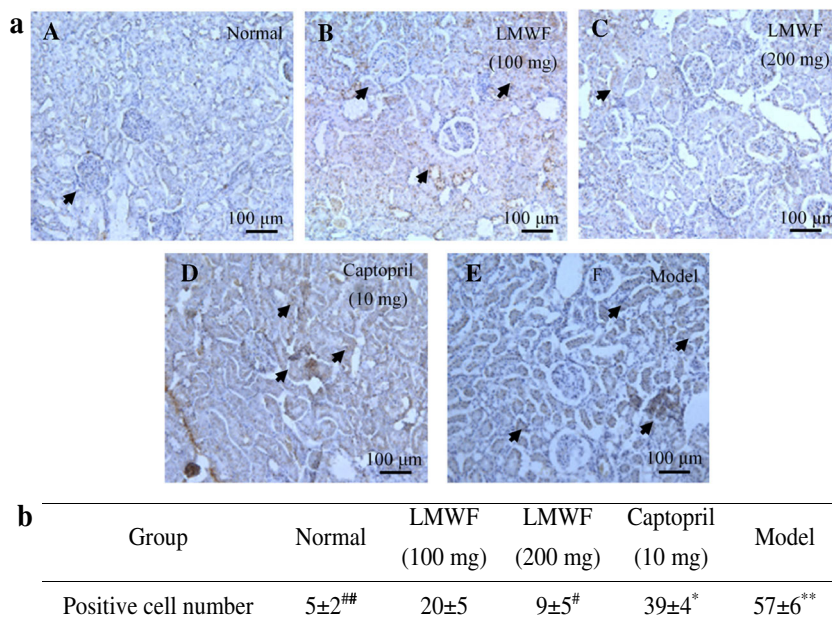

Fig. 10 Effect of LMWF on CTGF, VEGF, JNK, and P-JNK levels in DN rats kidney by western blot

significantly protected against diabetes-induced hypertension and hyperlipidemia (Cui et al. 2014). All of these data demonstrated that LMWF could significantly slow and prevent the progress of DN and protect the renal function in rats, which means that LMWF can ameliorate renal pathologic change of DN rats.

To further explore the effect of LMWF on renal pathologic changes of DN rats, we detected the content of glycosaminoglycan, AGER, and microstructure at the tissue and subcellular levels. Glycosaminoglycan has various biological functions and locations in cells; it can modulate growth factors and membrane filtration and serve as receptors in cell signaling (Conde-Knape 2001). It plays a key role in maintaining the normal GBM structure and filtration function and was involved in the transport of cells and small molecules across the GBM (Yung et al. 2013). HA is a typical glycosaminoglycan, LMWF has a similar structure to glycosaminoglycan, and we found that LMWF could reduce the HA content in urine (Fig. 5). It was demonstrated that LMWF could prevent glycosaminoglycan from abnormal degradation; in consequence, LMWF may protect the normal GBM structure and filtrating function and slow the development of DN.

Advanced glycosylation end product-specific receptor (AGER, also known as RAGE) is a multiligand receptor of the immunoglobulin superfamily. It interacts with distinct molecules that are implicated in homeostasis, development, and inflammation in diabetes. The multiple component of AGE-AGER can regulate signal transduction, ligands formation, pro-inflammatory responses, and GBM alternation; it can cause microvascular complications in diabetes (Yamagishi and Matsui 2010). Many inflammatory cytokines that contribute to DN are activated and induced by AGE. Some studies have shown that the end point effect of AGE-AGER would be a promising target for curing DN (Singh et al. 2014). Our work showed that LMWF significantly reduced the AGER level in

Fig. 11 LMWF reduced the expression of CTGF in DN rats kidneys. **a** (A) Representative images of the normal group by hematoxylin staining after immunohistochemistry, (B, C) groups administered with LMWF at doses of 100 and 200 mg kg^{-1} day^{-1} respectively, (D) captopril (10 mg) group, and (E) model group. *Black arrows* indicate the positive cell. *Scale bar* = 100 μm in each panel. **b** Positive cells were counted in five visual fields in one section. Data are expressed as means ± S.D. *Asterisk* $P < 0.05$, *double asterisk* $P < 0.01$ (vs normal group); *hash* $P < 0.05$, *double hash* $P < 0.01$ (vs model group)

Group	Normal	LMWF (100 mg)	LMWF (200 mg)	Captopril (10 mg)	Model
Positive cell number	5±2$^{\#\#}$	20±5	9±5$^{\#}$	39±4*	57±6**

the kidneys of DN rats (Fig. 8). LMWF downregulated inflammatory cytokines and improved microvascular complications in diabetes. Based on the pathologic changes that we observed in the DN rats (Figs. 6 and 7), the podocyte and endotheliocyte windows and the GBM of treated rats were much more structurally integrated. Thus, LMWF, especially LMWF (200 mg kg^{-1}), could ameliorate the degree of pathologic change and glomerular filtration function alteration.

Finally, to investigate the regulation of inflammatory cytokines by LMWF, we inspected statistically positive expressions of JNK, IL-6, VEGF, and CTGF in the kidneys of DN rats (Figs. 9, 10, and 11). AGE expression can activate and improve the VEGF of podocytes in the diabetic glomerulus in early diabetes. Increased expression of VEGF and IL-6 which are induced by VEGF in the kidneys of DN patients can stimulate angiogenesis, evaluate microvascular permeability, and attract inflammatory cells to the glomerulus. Those factors are also the cause of albuminuria and glomerulosclerosis in diabetes, especially in the early phase (Iozzo et al. 1997; Wendt et al. 2003). A blockade of VEGF can abolish hyper-filtration in the glomerulus and inhibit the increase of uAlb; thus, it may contribute to vascular permeability, functional and morphological alterations in DN. CTGF is a downstream target of TGF-β in DN and plays an important role in AGE-induced epithelial-to-mesenchymal differentiation. Suppression of CTGF expression may improve tubule glomerulosclerosis, albuminuria, and chronic hyperglycemia in DN patients (Burns et al. 2006). The JNK pathway can modulate the inflammatory cytokine signaling cascade in mesangial cells (Kanwar et al. 2011). Accord to our study, LMWF could inhibit the expression of the inflammatory cytokine mentioned above, relieving the inflammatory response in the kidneys of DN rats. And compared to LMWF (200 mg)

group, LMWF (100 mg) group relieved the inflammatory response more remarkably. Thus, both LMWF (100 mg kg^{-1}) and LMWF (200 mg kg^{-1}) could prevent AGE generation and accumulation in DN rats also protect HA from degradation, especially in LMWF (100 mg) group. It is able to maintain the integrity of GBM and improve the glomerular filtration function. Furthermore, LMWF relieves the inflammatory response through the signaling cascade.

However, different doses of LMWF may affect DN in various ways. High dose of LMWF (200 mg kg^{-1}) could inhibit body weight losing better than low dose of LMWF (100 mg kg^{-1}), the diagnostic indices of DN, such as M-TP and uAlb, and serum biochemical indexes levels in rats treated with high dose of LMWF were lower than that in rats treated with low dose of LMWF. Meanwhile, high dose of LMWF maintained more complete structure and function of glomerular basement membrane in DN rats. But low dose of LMWF decreased inflammatory cytokines expression more effectively.

In conclusion, LMWF reduced the levels of UREA and FRUC level in the blood, decreased M-TP and uAlb levels in the urine, maintained the structural integrity of the GBM and glomerulus, protected glycosaminoglycans from abnormal degradation, inhibited AGE generation and accumulation, and also suppressed the expression of inflammatory cytokines, such as JNK, IL-6, VEGF, and CTGF. Consequently, the therapeutic mechanism to diabetic nephropathy by LMWF is that LMWF improves the glomerular filtration function and modulates inflammatory response in kidney, and then ameliorates and slows down the development and progression of DN in rats. This study may provide a novel target and method for preventing and curing the diabetic nephropathy.

Author contributions Yingjie Xu designed the study, provided most of the data, and wrote the article; Quanbin Zhang co-authored the article and designed the study; Jing Wang co-did the experiments and provided some data; and Dali Luo and Delin Duan co-designed the study.

Compliance with ethical standards Experiments involving live animals were conducted in accordance with the "National Guide for the Care and Use of Laboratory Animals" and the "Regulations for the Administration of Affairs Concerning Experimental Animals" promulgated by the State Science and Technology Commission of Shandong Province. The study was approved by the ethics committee of Institute of Oceanology, Chinese Academy of Sciences.

Conflict of interest The authors declare that they have no conflict of interest.

References

Anastyuk SD, Shevchenko NM, Ermakova SP, Vishchuk OS, Nazarenko EL, Dmitrenok PS, Zvyagintseva TN (2012) Anticancer activity in vitro of a fucoidan from the brown alga *Fucus evanescens* and its low-molecular fragments, structurally characterized by tandem mass-spectrometry. Carbohydr Polym 87:186–194

Bachelet L, Bertholon I, Lavigne D, Vassy R, Jandrot-Perrus M, Chaubet F, Letourneur D (2009) Affinity of low molecular weight fucoidan for P-selectin triggers its binding to activated human platelets. Biochim Biophys Acta 1790:141–146

Bishop JR, Schuksz M, Esko JD (2007) Heparan sulphate proteoglycans fine-tune mammalian physiology. Nature 446:1030–1037

Burns WC, Twigg SM, Forbes JM, Pete J, Tikellis C, Thallas-Bonke V, Thomas MC, Cooper ME, Kantharidis P (2006) Connective tissue growth factor plays an important role in advanced glycation end product-induced tubular epithelial-to-mesenchymal transition: implications for diabetic renal disease. J Am Soc Nephrol 17:2484–2494

Chen J, Wang W, Zhang Q, Li F, Lei T, Luo D, Zhou H, Yang B (2013) Low molecular weight fucoidan against renal ischemia-reperfusion injury via inhibition of the MAPK signaling pathway. PLoS One 8: e56224

Conde-Knape K (2001) Heparan sulfate proteoglycans in experimental models of diabetes: a role for perlecan in diabetes complications. Diabetes Metab Res Rev 17:412–421

Costa LS, Fidelis GP, Cordeiro SL, Oliveira RM, Sabry DA, Camara RB, Nobre LT, Costa MS, Almeida-Lima J, Farias EH, Leite EL, Rocha HA (2010) Biological activities of sulfated polysaccharides from tropical seaweeds. Biomed Pharmacother 64:21–28

Cui W, Zheng Y, Zhang Q, Wang J, Wang L, Yang W, Guo C, Gao W, Wang X, Luo D (2014) Low-molecular-weight fucoidan protects endothelial function and ameliorates basal hypertension in diabetic Goto-Kakizaki rats. Lab Investig 94:382–393

Deux JF, Meddahi-Pellé A, Le Blanche AF, Feldman LJ, Colliec-Jouault S, Brée F, Boudghène F, Michel JB, Letourneur D (2002) Low

molecular weight fucoidan prevents neointimal hyperplasia in rabbit iliac artery in-stent restenosis model. Arterioscler Thromb Vasc Biol 22:1604–1609

Durand E, Helley D, Al Haj Zen A, Dujols C, Bruneval P, Colliec-Jouault S, Fischer AM, Lafont A (2008) Effect of low molecular weight fucoidan and low molecular weight heparin in a rabbit model of arterial thrombosis. J Vasc Res 45:529–537

Durig J, Bruhn T, Zurborn K, Gutensohn K, Bruhn H, Beress L (1997) Anticoagulant fucoidan fractions from *Fucus vesiculosus* induce platelet activation in vitro. Thromb Res 85:479–491

Fan WX, Deng ZX, Liu F, Liu RB, He L, Amrit B, Zang L, Li JW, Liu XR, Huang SM, et al. (2012) Spontaneous retroperitoneal hemorrhage after hemodialysis involving anticoagulant agents. J Zhejiang Univ Sci B 13:408–412

Group IDFDA (2015)) Update of mortality attributable to diabetes for the IDF Diabetes Atlas: estimates for the year 2013. In Diabetes Res Clin Pract 109:461–465

Haraldsson B, Nystrom J, Deen W (2008) Properties of the glomerular barrier and mechanisms of proteinuria. Physiol Rev 88:451–487

Hemmingson JA, Falshaw R, Furneaux RH, Thompson K (2006) Structure and antiviral activity of the galactofucan sulfates extracted from *Undaria pinnatifida* (Phaeophyta). J Appl Phycol 18:185–193

Hlawaty H, Suffee N, Sutton A, Oudar O, Haddad O, Ollivier V, Laguillier-Morizot C, Gattegno L, Letourneur D, Charnaux N (2011) Low molecular weight fucoidan prevents intimal hyperplasia in rat injured thoracic aorta through the modulation of matrix metalloproteinase-2 expression. Biochem Pharmacol 81:233–243

Iozzo R, Pillarisetti J, Sharma B, Murdoch AD, Danielson KG, Uitto J, Mauviel A (1997) Structural and functional characterization of the human perlecan gene promoter. Transcriptional activation by transforming growth factor-beta via a nuclear factor 1-binding element. J Biol Chem 272:5219–5228

Jiao G, Yu G, Zhang J, Ewart HS (2011) Chemical structures and bioactivities of sulfated polysaccharides from marine algae. Mar Drugs 9: 196–223

Jin W, Wang J, Jiang H, Song N, Zhang W, Zhang Q (2013) The neuroprotective activities of heteropolysaccharides extracted from *Saccharina japonica*. Carbohydr Polym 97:116–120

Li J, Qu X, Yao J, Caruana G, Ricardo SD, Yamamoto Y, Yamamoto H, Bertram JF (2010) Blockade of endothelial-mesenchymal transition by a Smad3 inhibitor delays the early development of streptozotocin-induced diabetic nephropathy. Diabetes 59:2612–2624

Kanasaki K, Taduri G, Koya D (2013) Diabetic nephropathy: the role of inflammation in fibroblast activation and kidney fibrosis. Front Endocrinol 4:7

Kanwar YS, Sun L, Xie P, Liu FY, Chen S (2011) A glimpse of various pathogenetic mechanisms of diabetic nephropathy. Annu Rev Pathol 6:395–423

Kashihara N, Haruna Y, Kondeti VK, Kanwar YS (2010) Oxidative stress in diabetic nephropathy. Curr Med Chem 17:4256–4269

Lim AK, Tesch GH (2012) Inflammation in diabetic nephropathy. Mediat Inflamm 2012:146154

Ma J, Wu H, Zhao CY, Panchapakesan U, Pollock C, Chadban SJ (2014) Requirement for TLR2 in the development of albuminuria, inflammation and fibrosis in experimental diabetic nephropathy. Int J Clin Exp Pathol 7:481–495

Matsushita Y, Ogawa D, Wada J, Yamamoto N, Shikata K, Sato C, Tachibana H, Toyota N, Makino H (2011) Activation of peroxisome proliferator-activated receptor delta inhibits streptozotocin-induced diabetic nephropathy through anti-inflammatory mechanisms in mice. Diabetes 60:960–968

McCarthy KJ, Wassenhove-McCarthy DJ (2012) The glomerular basement membrane as a model system to study the bioactivity of heparan sulfate glycosaminoglycans. Microsc Microanal 18:3–21

Nardella A, Chaubet F, BoissonVidal C, Blondin C, Durand P, Jozefonvicz J (1996) Anticoagulant low molecular weight fucans

produced by radical process and ion exchange chromatography of high molecular weight fucans extracted from the brown seaweed *Ascophyllum nodosum*. Carbohydr Res 289:201–208

Naylor RN, Greeley SA, Bell GI, Philipson LH (2011) Genetics and pathophysiology of neonatal diabetes mellitus. J Diabetes Investig 2:158–169

Nazir K, Siddiqui K, Al-Qasim S, Al-Naqeb D (2014) Meta-analysis of diabetic nephropathy associated genetic variants in inflammation and angiogenesis involved in different biochemical pathways. BMC Med Genet 15:103

Pal PB, Sinha K, Sil PC (2014) Mangiferin attenuates diabetic nephropathy by inhibiting oxidative stress mediated signaling cascade, TNFalpha related and mitochondrial dependent apoptotic pathways in streptozotocin-induced diabetic rats. PLoS One 9:e107220

Pan Y, Huang Y, Wang Z, Fang Q, Sun Y, Tong C, Peng K, Wang Y, Miao L, Cai L, Zhao Y, Liang G (2014) Inhibition of MAPK-mediated ACE expression by compound C66 prevents STZ-induced diabetic nephropathy. J Cell Mol Med 18:231–241

Papale M, Papale M, Di Paolo S, Magistroni R, Lamacchia O, Di Palma AM, De Mattia A, Rocchetti MT, Furci L, Pasquali S, De Cosmo S, Cignarelli M, Gesualdo L (2010) Urine proteome analysis may allow noninvasive differential diagnosis of diabetic nephropathy. Diabetes Care 33:2409–2415

Remuzzi G, Schieppati A, Ruggenenti P (2002) Nephropathy in patients with type 2 diabetes. N Engl J Med 346:1145–1151

Rossini M, Naito T, Yang H, Freeman M, Donnert E, Ma LJ, Dunn SR, Sharma K, Fogo AB (2010) Sulodexide ameliorates early but not late kidney disease in models of radiation nephropathy and diabetic nephropathy. Nephrol Dial Transplant 25:1803–1810

Sakagami Y, Nakajima M, Takagawa K, Ueda T, Akazawa H, Maruhashi Y, Shimoyama H, Kamitsuji H, Yoshioka A (2004) Analysis of glomerular anionic charge status in children with IgA nephropathy using confocal laser scanning microscopy. Nephron Clin Pract 96:c96–c104

Satchell SC, Braet F (2009) Glomerular endothelial cell fenestrations: an integral component of the glomerular filtration barrier. Am J Physiol Renal Physiol 296:F947–F956

Sawa Y, Takata S, Hatakeyama Y, Ishikawa H, Tsuruga E (2014) Expression of toll-like receptor 2 in glomerular endothelial cells and promotion of diabetic nephropathy by *Porphyromonas gingivalis* lipopolysaccharide. PLoS One 9:e0097165

Singh A, Satchell SC, Neal CR, McKenzie EA, Tooke JE, Mathieson PW (2007) Glomerular endothelial glycocalyx constitutes a barrier to protein permeability. J Am Soc Nephrol 18:2885–2893

Singh VP, Bali A, Singh N, Jaggi AS (2014) Advanced glycation end products and diabetic complications. Korean J Physiol Pharmacol 18:1–14

Takahashi S, Watanabe S, Wada N, Murakami H, Funaki S, Yan K, Kondo Y, Harada K, Nagata M (2006) Charge selective function in childhood glomerular diseases. Pediatr Res 59:336–340

Terami N, Ogawa D, Tachibana H, Hatanaka T, Wada J, Nakatsuka A, Eguchi J, Horiguchi CS, Nishii N, Yamada H, Takei K, Makino H (2014) Long-term treatment with the sodium glucose cotransporter 2 inhibitor, dapagliflozin, ameliorates glucose homeostasis and diabetic nephropathy in db/db mice. PLoS One 9:e100777

Tomita H, Sanford RB, Smithies O, Kakoki M (2012) The kallikrein-kinin system in diabetic nephropathy. Kidney Int 81:733–744

Vlassara H, Striker GE (2011) AGE restriction in diabetes mellitus: a paradigm shift. Nat Rev Endocrinol 7:526–539

Wang CZ, Ho ML, Chen WC, Chiu CC, Hung YL, Wang CK, Wu SC (2011a) Characterization and enhancement of chondrogenesis in porous hyaluronic acid-modified scaffolds made of PLGA(75/25)

blended with PEI-grafted PLGA(50/50). Mar Sci Eng C 31:1343–1351

Wang J, Liu H, Li N, Zhang Q, Zhang H (2014) The protective effect of fucoidan in rats with streptozotocin-induced diabetic nephropathy. Mar Drugs 12:3292–3306

Wang J, Wang F, Yun H, Zhang H, Zhang Q (2012) Effect and mechanism of fucoidan derivatives from *Laminaria japonica* in experimental adenine-induced chronic kidney disease. J Ethnopharmacol 139:807–813

Wang J, Zhang Q, Jin W, Niu X, Zhang H (2011b) Effects and mechanism of low molecular weight fucoidan in mitigating the peroxidative and renal damage induced by adenine. Carbohydr Polym 84:417–423

Wang J, Zhang Q, Zhang Z, Li Z (2008) Antioxidant activity of sulfated polysaccharide fractions extracted from *Laminaria japonica*. Int J Biol Macromol 42:127–132

Wang J, Zhang Q, Zhang Z, Song H, Li P (2010a) Potential antioxidant and anticoagulant capacity of low molecular weight fucoidan fractions extracted from *Laminaria japonica*. Int J Biol Macromol 46:6–12

Wang J, Zhang Q, Zhang Z, Zhang H, Niu X (2010b) Structural studies on a novel fucogalactan sulfate extracted from the brown seaweed *Laminaria japonica*. Int J Biol Macromol 47:126–131

Weil EJ, Lemley KV, Mason CC, Yee B, Jones LI, Blouch K, Lovato T, Richardson M, Myers BD, Nelson RG (2012) Podocyte detachment and reduced glomerular capillary endothelial fenestration promote kidney disease in type 2 diabetic nephropathy. Kidney Int 82:1010–1017

Wendt TM, Tanji N, Guo J, Kislinger TR, Qu W, Lu Y, Bucciarelli LG, Rong LL, Moser B, Markowitz GS, Stein G, Bierhaus A, Liliensiek B, Arnold B, Nawroth PP, Stern DM, D'Agati VD, Schmidt AM (2003) RAGE drives the development of glomerulosclerosis and implicates podocyte activation in the pathogenesis of diabetic nephropathy. Am J Pathol 162:1123–1137

Wijesekara I, Pangestuti R, Kim SK (2011) Biological activities and potential health benefits of sulfated polysaccharides derived from marine algae. Carbohydr Polym 84:14–21

Yamagishi S, Matsui T (2010) Advanced glycation end products, oxidative stress and diabetic nephropathy. Oxidative Med Cell Longev 3:101–108

Yu X, Zhang Q, Cui W, Zeng Z, Yang W, Zhang C, Zhao H, Gao W, Wang X, Luo D (2014) Low molecular weight fucoidan alleviates cardiac dysfunction in diabetic Goto-Kakizaki rats by reducing oxidative stress and cardiomyocyte apoptosis. J Diabetes Res 2014:420929

Yung S, Chau M, Zhang Q, Zhang C, Chan T (2013) Sulodexide decreases albuminuria and regulates matrix protein accumulation in C57BL/6 mice with streptozotocin-induced type I diabetic nephropathy. PLoS One 8:e54501

Zhang MZ, Wang S, Yang S, Yang H, Fan X, Takahashi T, Harris RC (2012) Role of blood pressure and the renin-angiotensin system in development of diabetic nephropathy (DN) in eNOS-/- db/db mice. Am J Physiol Renal Physiol 302:F433–F438

Zhang Z, Teruya K, Eto H, Shirahata S (2013) Induction of apoptosis by low-molecular-weight fucoidan through calcium- and caspase-dependent mitochondrial pathways in MDA-MB-231 breast cancer cells. Biosci Biotech Biochem 77:235–242

Zhu Z, Zhang Q, Chen L, Ren S, Xu P, Tang Y, Luo D (2010) Higher specificity of the activity of low molecular weight fucoidan for thrombin-induced platelet aggregation. Thromb Res 125:419–426